Monte Carlo simulations of rigid biopolymer growth processes

Cite as: J. Chem. Phys. **123**, 124902 (2005); https://doi.org/10.1063/1.2013248
Submitted: 25 April 2005 • Accepted: 11 July 2005 • Published Online: 23 September 2005

Jenny Son, G. Orkoulas and Anatoly B. Kolomeisky

Monte Carlo simulations of rigid biopolymer growth processes

Jenny Son and G. Orkoulas[a)]
Department of Chemical and Biomolecular Engineering, University of California, Los Angeles, California 90095

Anatoly B. Kolomeisky
Department of Chemistry, Rice University, Houston, Texas 77005

(Received 25 April 2005; accepted 11 July 2005; published online 23 September 2005)

Rigid biopolymers, such as actin filaments, microtubules, and intermediate filaments, are vital components of the cytoskeleton and the cellular environment. Understanding biopolymer growth dynamics is essential for the description of the mechanisms and principles of cellular functions. These biopolymers are composed of N parallel protofilaments which are aligned with arbitrary but fixed relative displacements, thus giving rise to complex end structures. We have investigated rigid biopolymer growth processes by Monte Carlo simulations by taking into account the effects of such "end" properties and lateral interactions. Our simulations reproduce analytical results for the case of $N=2$, which is biologically relevant for actin filaments. For the case of $N=13$, which applies to microtubules, the simulations produced results qualitatively similar to the $N=2$ case. The simulation results indicate that polymerization events are evenly distributed among the N protofilaments, which imply that both end-structure effects and lateral interactions are significant. The effect of different splittings in activation energy has been investigated for the case of $N=2$. The effects of activation energy coefficients on the specific polymerization and depolymerization processes were found to be unsubstantial. By expanding the model, we have also obtained a force-velocity relationship of microtubules as observed in experiments. In addition, a range of lateral free-energy parameters was found that yields growth velocities in accordance with experimental observations and previous simulation estimates for the case of $N=13$. © *2005 American Institute of Physics*.
[DOI: 10.1063/1.2013248]

I. INTRODUCTION

Rigid biopolymers are vital components of the cytoskeleton and the cellular environment. Microtubules, actin filaments, and intermediate filaments are such rigid biopolymers that play a fundamental role in biological systems by facilitating cellular transport, cell motility, and reproduction.[1,2] These cytoskeletal biopolymers polymerize and depolymerize, and also move within the cytoplasm.[1,2] Polymerization and depolymerization processes display the phenomenon of recurrent growing and shrinking phases which alternate stochastically. This is termed "dynamic instability" and it enables the growing microtubules to explore space and reorganize.[3] Although the behavior of microtubules in living cells can be attributed to dynamic instabilities, the exact mechanisms and biological functions are not completely known.

Microtubules are rigid, cylindrical tubes with diameter of approximately 25 nm that are composed of N parallel protofilaments. N varies from 10–15, but typically $N=13$ is most prevalent for the ones that are nucleated from centrosomes.[4] Polymerization and depolymerization dynamics of microtubules have been studied extensively, both experimentally and theoretically. Experimental measurements of growth dynamics of actin filaments and microtubules under external forces have been made,[5–7] and theoretical models, such as polymer ratchet[8,9] and phenomenological[10,11] models, have been proposed. Despite the fact that the theoretical models provide adequate descriptions of the dynamics of growing rigid biopolymers, they lack information on microscopic structure, geometrical properties of a biopolymer's lattice, and lateral interactions between protofilaments.[12,13] Computer simulations have also been employed for the study of microtubule dynamics.[14] These simulations do not describe accurately the geometry of the growing ends in microtubules.

Stukalin and Kolomeisky[12] developed a model which takes into account the complex structure of the growing end of the biopolymer and obtained analytical solutions for the case of $N=2$, which is relevant to actin filaments. In Ref. 12, two models for microtubule growth were considered, "one-layer" and "full" model, respectively. In the one-layer model, the distances between the tips of the protofilaments are constrained to lie within one subunit length in the allowed polymer configurations. In contrast, the full model has no such restriction. Despite the fact that the one-layer model is soluble[15] for arbitrary N, analytical solutions cannot be obtained for the cases of $N=10-15$, which are relevant to microtubules, for the full model. Analytical difficulties arise due to the enormous number of configurations associated with $N>2$. The objective of this work is to perform Monte Carlo simulations to obtain results for the growth velocities for the analytically insoluble cases of $N>2$ full model in

[a)]Electronic mail: makis@seas.ucla.edu

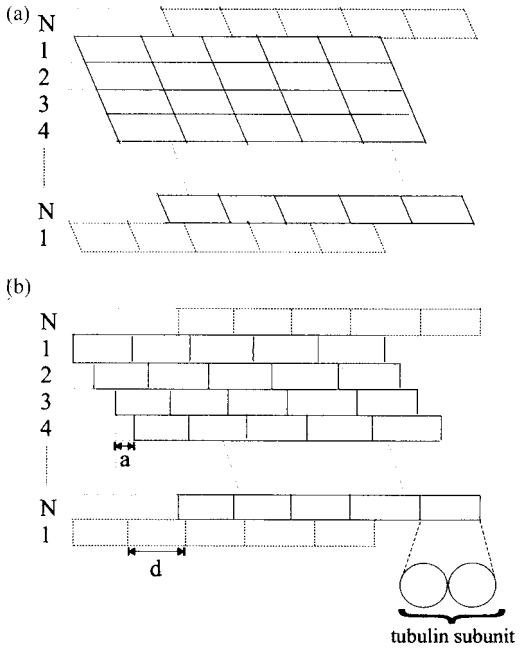

FIG. 1. Matrix diagram. (a) The tip of the microtubule is flat. (b) The tip of the microtubule shows jagged edges.

order to test how well the one-layer approximation describes the growth of rigid biopolymers, as well as to study the effects of activation energy coefficients for specific polymerization/depolymerization processes. For the case in which the activation energy coefficients are nonzero, the models considered in Ref. 12 cannot be solved analytically. Furthermore, for the $N=13$ full model, we have found a range of lateral energy parameters that yields growth velocities consistent with experimental observations[5] and previous simulations.[14] In addition, since growing microtubules are known to generate forces,[2,3,5] we have obtained a force-velocity curve which is in good accord with experimental measurements[5] for the analytically intractable $N=13$ full model. The difference between our work and previous simulations is that we incorporated the shift distance a between adjacent protofilaments in order to explicitly calculate the magnitude of lateral interactions, whereas previous work did not focus on these microscopic details.

II. DESCRIPTION OF THE MODEL

The parallel protofilaments of microtubules are polymers and their building blocks are globular proteins called tubulin subunits. Tubulin subunits are heterodimers that are composed of alternating α- and β-tubulin monomers, see Fig. 1(b). Because of the head-to-tail arrangement of the α- and β-tubulin subunits in protofilaments, polarity arises and the (+)– end displays a faster rate of growth than the (−)– end. In this work, we consider microtubule growth from the (+)– end only. However, the method of assembly at both ends are analogous, and recently, growth dynamics of rigid two-stranded polymers at both ends has been described as a combination of growth processes at each end separately.[16]

Whereas previous Monte Carlo simulations on microtubule growth dynamics did not take into account the jagged edges of the growing end of the biopolymer,[14] the present work incorporates the detailed microscopic structure in the model, see Fig. 1. Note the omission of the jagged growing end of the microtubule in Fig. 1(a). In this schematic, the "surface" of the microtubule tip is flat, whereas in reality, it displays some "surface roughness." In contrast, note the details of the rough edges in Fig. 1(b). The length of the tubulin subunit is $d=8.2$ nm, and a is the shifted distance for adjacent protofilaments. Figure 1(b) is a much more realistic representation of a microtubule of a B-type lattice with a seam.[2] Note that each rectangular tubulin subunit represents a dimer of alternating α- and β- monomers. Specific to this diagram, the Nth protofilament is termed the "leading" protofilament because it is the longest.

The hollow, cylindrical nature of microtubule is simulated by mimicking a contact between the first and last columns (protofilament 1 and N), see Fig. 1. Adjacent protofilaments are shifted by an arbitrary distance a. For real microtubules with $N=13$, $a=0.96$ nm. However, in the simplified symmetric case where seam effects are not explicitly taken into account, a can be estimated as $d/13$ or $a=0.63$ nm. The jagged tip of the growing biopolymer can be treated as a surface, where structural roughness arises from attachment or detachment of individual subunits.[17] A variable M_i is introduced as a measure of the exposed surface and molecular roughness. It represents the lateral interactions that an incoming subunit will have with its adjacent protofilaments. We explicitly calculate $[M_1, M_2, \ldots, M_i, \ldots, M_{N-1}, M_N]$ for each ith protofilament. In essence, M_i are the sums of the differences in lengths (x_i) of protofilaments that are on either side of protofilament i, i.e.,

$$M_i = |x_{i-1} - x_i| + |x_i - x_{i+1}| \tag{1}$$

and

$$m_i = \frac{M_i}{d}, \tag{2}$$

where Eq. (2) represents the fraction of lateral interactions that an incoming subunit will have.[18]

It is known that microtubule assembly is not diffusion-limited when the tubulin subunits approach the growing biopolymer.[19] Therefore, it follows that a careful investigation of the rates of attachment (r_{ai}) and detachment (r_{di}), which are in turn influenced by the complex structure of the growing end, the geometrical properties, and the lateral interactions between the protofilaments, is necessary in order to evaluate the long-time mean velocity. These rates are related by the following thermodynamic expression:[12]

$$\frac{r_{ai}/c}{r_{di}} = e^{-(g_v + g_{im} + g_{hi})/k_B T}, \tag{3}$$

where $c=25$ μM is the concentration of free tubulin subunits used in experiments.[5] Note that the appearance of c arises because the rate of attachment is proportional to the concentration of free subunits. In Eq. (3), g_v is the vertical bond energy, g_{im} is the energy for immobilizing tubulin subunits into the rigid lattice, and g_{hi} is the lateral bond energy. Note that these energies are negative, which is an implication of weak chemical bonds (microtubules are noncovalent

polymers[2]). The head-to-tail binding (vertical) and immobilization energies are constant for any configuration, whereas the lateral energy varies depending on the local configuration at the tip of the growing microtubule. Then the lateral energy for the ith protofilament is expressed by the following:

$$g_{hi} = m_i g_{ho}, \tag{4}$$

where g_{ho} is a constant and m_i is the measure of the fraction of lateral interactions for site i. Subsequently, the rates of attachment and detachment can be written as follows:

$$r_{ai} \propto e^{-\theta(g_v+g_{im}+g_{hi})/k_BT}, \tag{5}$$

$$r_{di} \propto e^{-(\theta-1)(g_v+g_{im}+g_{hi})/k_BT}. \tag{6}$$

In Eqs. (5) and (6), θ reflects the value of the activation barrier for subunit binding, $0<\theta<1$.[12]

Attachment and detachment rates for the leading protofilament (R_a and R_d, respectively) have no dependence on g_{hi}, and they can be represented by the following expressions for any configuration:[12]

$$\frac{R_d/c}{R_d} = e^{-(g_v+g_{im})/k_BT}. \tag{7}$$

Then rates r_{ai} and r_{di} for protofilaments other than the leading one can be expressed by the following:

$$\frac{r_{ai}}{r_{di}} = \frac{R_a}{R_d}\gamma^{m_i}, \tag{8}$$

where

$$\gamma = e^{-g_{ho}/k_BT} \tag{9}$$

is the lateral energy parameter. The thermodynamic expression in Eq. (8) can be rewritten in the following form:

$$r_{ai} = R_a\gamma^{f_i+(1/2)m_i}, \tag{10}$$

$$r_{di} = R_d\gamma^{f_i-(1/2)m_i}. \tag{11}$$

The coefficients f_i reflect the different values of activation energies for specific polymerization and depolymerization processes. In this work we first consider the case $f_i=0$ for the purpose of comparing our results to those of analytical results. After successful reproduction of the analytical results, f_i will be explicitly determined for each protofilament under the following criteria:[12]

$$-\tfrac{1}{2}m_i < f_i < \tfrac{1}{2}m_i \tag{12}$$

or

$$-1 < f_i < 1. \tag{13}$$

Equation (12) applies to protofilaments for which the tips are at a distance less than d from the adjacent protofilaments,[20] and Eq. (13) applies to protofilaments for which the tips are at a distance greater than d from the adjacent protofilaments.

The coefficients f_i are related to the amount of lateral interactions that the incoming subunits will have based on the configurations of their adjacent protofilaments [Eqs. (12) and (13)]. Since these coefficients imply a faster attachment to the protofilament where a stronger lateral bond is created, and conversely, a slower dissociation where a stronger lateral bond is to be broken, it is necessary to investigate the degree of significance of their effects on the growth velocities of the microtubules.

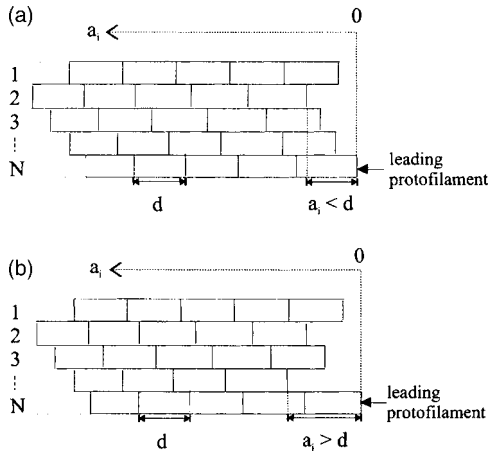

FIG. 2. (a) One-layer model of the rigid polymer. (b) Full model of the rigid polymer.

In Ref. 12 two different models of growth were proposed: the one-layer model and the full model. Consider a growing rigid polymer in Fig. 2. The location of the leading protofilament (the longest protofilament) is where $a_i=0$. Using this as a reference, the one-layer model corresponds to $a_i<d$ for protofilaments other than the leading one, see Fig. 2(a). The absence of the constraint $a_i<d$ corresponds to the so-called full model, see Fig. 2(b). The ratio of the velocities of these two models are obtained in order to determine how well the simple one-layer model describes the more realistic full model.

III. SIMULATION METHODOLOGY

The growth of microtubules is a nonequilibrium process and it is thus simulated by a kinetic Monte Carlo method. Kinetic Monte Carlo algorithms are based on a dynamic interpretation of the Monte Carlo method through the master equation.[21–24] They were developed to address the questions of convergence and accuracy of the Monte Carlo method[22] and they also formed the basis for applying the Monte Carlo method to simulate dynamic processes.[25] In this work, the growth of microtubules is simulated by a kinetic Monte Carlo algorithm that was developed for Ising systems with nearest-neighbor interactions[23] and extended in stochastic formulations of chemical reactions[26–28] by Gillespie. The transient behavior of a system that executes a random walk over a discrete set of states $\{S_1, S_2, \ldots, S_m, \ldots, S_n, \ldots\}$ is described by the master equation:

$$\frac{dP^{(n)}(t)}{dt} = \sum_m P^{(m)}(t)\cdot W_{mn} - \sum_m P^{(n)}(t)\cdot W_{nm}, \tag{14}$$

where $P^{(n)}(t)$ is the probability that the system is in state S_n at time t and W_{mn} is the transition probability per unit time from state S_m to S_n. Even for cases for which the transition probabilities do not have explicit time dependence (as it is

the case in this work), the master equation Eq. (14) is analytically and numerically intractable. An equivalent description of the random walk, well-suited for numerical implementations, may be formulated through the transition probability density function $P_n(\tau|m,t)$.[27] Given that the system is at state S_m at time t, $P_n(\tau|m,t)d\tau$ is the probability that the system "hops" to state S_n in the time interval $(t+\tau, t+\tau+d\tau)$. $P_n(\tau|m,t)$ is written as[27]

$$P_n(\tau|m,t)d\tau = \tilde{P}_0(\tau|m,t)\cdot W_{mn}d\tau, \tag{15}$$

where $\tilde{P}_0(\tau|m,t)$ is the probability that no transition occurs in the time interval $(t,t+\tau)$ (i.e., the system stays in state S_m) and $W_{mn}d\tau$ is the probability that the system moves from S_m to S_n in the time interval $(t+\tau, t+\tau+d\tau)$. The waiting-time probability $\tilde{P}_0(\tau|m,t)$ satisfies the following identity:

$$\tilde{P}_0(\tau+d\tau|m,t) = \tilde{P}_0(\tau|m,t)\cdot(1-W_m d\tau), \tag{16}$$

where

$$W_m = \sum_n W_{mn}, \tag{17}$$

and $W_m d\tau$ is the probability that the system moves away from state S_m within $d\tau$. Rearrangement of Eq. (16) yields

$$\frac{d\tilde{P}_0(\tau|m,t)}{\tilde{P}_0(\tau|m,t)} = -W_m d\tau, \tag{18}$$

which can be integrated subject to $\tilde{P}_0(0|m,t)=1$ to give

$$\tilde{P}_0(\tau|m,t) = e^{-W_m\tau}. \tag{19}$$

Using Eqs. (15) and (19), the transition probability density $P_n(\tau|m,t)$ can be explicitly written as

$$P_n(\tau|m,t) = W_{mn}e^{-W_m\tau}. \tag{20}$$

For continuous-time/discrete-state random walks, it is more convenient to express $P_n(\tau|m,t)$ in the following form:[27]

$$P_n(\tau|m,t)d\tau = \tilde{P}_1(\tau|m,t)d\tau\cdot\pi_{mn}, \tag{21}$$

where $\tilde{P}_1(\tau|m,t)d\tau$ is the probability that a transition from state S_m to another state (any one) occurs in $(t+\tau, t+\tau+d\tau)$ and π_{mn} is the "hopping" probability from S_m to S_n. $\tilde{P}_1(\tau|m,t)$ and π_{mn} are given by

$$\tilde{P}_1(\tau|m,t) = \sum_n P_n(\tau|m,t) = W_m e^{-W_m\tau}, \tag{22}$$

$$\pi_{mn} = \frac{P_n(\tau|m,t)}{\tilde{P}_1(\tau|m,t)} = \frac{W_{mn}}{W_m}. \tag{23}$$

In the implementation of the random walk under consideration, given that the system is at state S_m at time t, one must determine at what time $t+\tau$ the next step occurs and to which state S_n the system jumps. The specification of the time increment τ and the state S_n (or the integer n) is done according to the transition probability density function $P_n(\tau|m,t)$ and it is based on the fact that the two-variable function $P_n(\tau|m,t)$ can be written as the product of two one-variable functions, $\tilde{P}_1(\tau|m,t)$ and π_{mn}, respectively, see Eq. (21). First, a state S_n or equivalently an integer n is selected with probability π_{mn}. Let

$$F_m(n) = \sum_{j=1}^{n}\pi_{mj} \tag{24}$$

be the probability that $k \leqslant n$, where k is the number of several independent paths stemming from state S_m.[26] If ξ_1 is a random number uniformly distributed in [0, 1), then integer n (and state S_n) is selected if the following inequality is satisfied:[29,30]

$$F_m(n-1) \leqslant \xi_1 < F_m(n). \tag{25}$$

A time increment τ must also be generated from the probability density $\tilde{P}_1(\tau|m,t)$. To this end, consider the probability distribution $\tilde{F}_1(\tau|m,t)$ defined by

$$\tilde{F}_1(\tau|m,t) = \int_0^\tau d\eta\tilde{P}_1(\eta|m,t) = 1 - e^{-W_m\tau}. \tag{26}$$

If ξ_2 is a random number uniformly distributed in [0, 1), τ is found from $\tilde{F}_1(\tau|m,t)=\xi_2$ or

$$\tau = -\frac{1}{W_m}\ln(1-\xi_2), \tag{27}$$

which ensures that τ is distributed according to the probability density $\tilde{P}_1(\tau|m,t)$. Statistical averages are obtained by performing several independent realizations of the random walk according to the previous methodology. In the microtubule growth problem, a state S_m is characterized by a given arrangement of the protofilaments and a new state is obtained by adding or removing a tubulin subunit. If N is the number of protofilaments, the total number of states within reach of the current state is $2N$.[31] The $2N$ hopping probabilities π_{mn} are defined by

$$\pi_{mn} = \frac{r_n}{\sum_{j=1}^{2N} r_j}, \tag{28}$$

where r_n is either the rate of attachment or detachment (r_{ai} or r_{di} [Eq. (10) or (11)], respectively) of a tubulin monomer to a given protofilament.

IV. RESULTS AND DISCUSSION

We have performed Monte Carlo simulations for the cases of $N=2$ and $N=13$ for both models, one-layer and full, respectively. In the simulations we evaluate the asymptotic (long-time) mean growth velocity

$$\langle x(t)\rangle \approx Vt, \tag{29}$$

where $x(t)$ represents the length of the biopolymer at time t. This length is the maximum value among the N protofilaments at time t in order to be consistent with the methods of experimental measurements. Our first goal is to reproduce the velocities obtained in Ref. 12 with zero activation energy coefficients f_i for $N=2$. The growth velocity of the microtubule is determined by calculating the statistical average $\langle x(t)\rangle$ as a function of time, see Fig. 7 below. Our results are shown

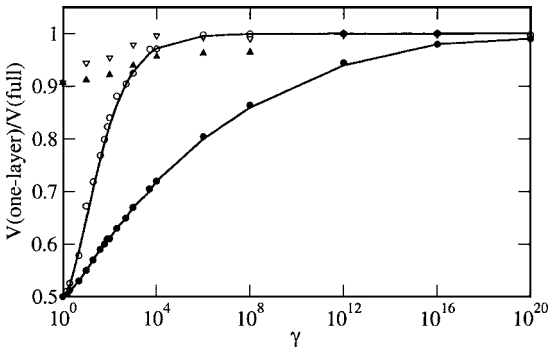

FIG. 3. Ratio of mean growth velocities V(one-layer)$/V$(full) for the cases of $N=2$ and $N=13$ as functions of the lateral energy parameter γ. (○) shows simulation results for $N=2$, $a/d=0.6$, and (●) shows simulation results for $N=2$, $a/d=0.1$. The solid lines are the analytical predictions of Ref. 12 for corresponding values of a/d. (▲) shows points for $N=13$, $a/d=0.1$, and (▽) shows points for $N=13$, $a/d=0.6$. The trend for $N=13$ is similar to $N=2$ model.

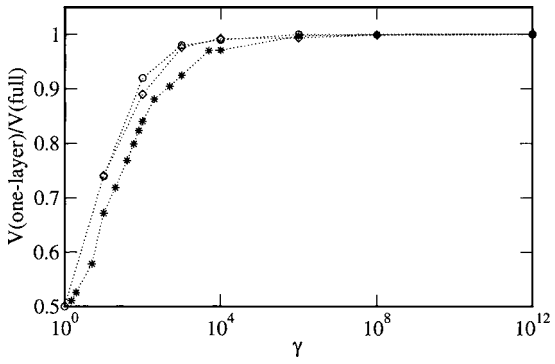

FIG. 4. Comparison of the ratios of mean growth velocities V(one-layer)$/V$(full) for the case of $N=2$ as functions of the lateral energy parameter γ for nonzero activation energy coefficients f_i. (∗) shows the results for $f_i=0$, (◇) is for positive and negative f_i, and (○) is for only positive f_i.

in Fig. 3 and are compared with the analytical predictions of Ref. 12. Figure 3 shows that the simulations reproduce the analytical results consistently. Note that the larger protofilament shift distance ($a/d=0.6$) results in better agreement for the one-layer and the full model. This is so because more favorable lateral bonds are created for $a/d=0.6$, due to the fact that more contact length is created between the incoming tubulin subunit and the protofilaments that are adjacent to the site of event.

The ratio of mean growth velocities for the case of $N=13$ is expected to display characteristics similar to the $N=2$ case. Results for the growth velocities for $N=13$ are shown in Fig. 3. The mean growth velocity ratio at $\gamma=1$ is 0.907 for both $a/d=0.1$ and 0.6, which is higher than the value of 0.5 for the case of $N=2$ for the same value of γ. This means that the one-layer model not only describes the dynamics of growth adequately for the $N=13$ model, but also it is a better description of growth for larger N. This behavior is as expected since there are more sites to choose from, and the event is more likely to be distributed evenly among the 13 possible sites. The ratio of mean growth velocities approaches the value of 1 for large values of γ and follows the trend of $N=2$. The one-layer model is thus an excellent description of the more realistic full model.

Whereas the results in Fig. 3 were obtained by assuming the activation energy coefficients to be zero,[12] Fig. 4 shows results for the cases of $N=2$, where the activation energy coefficients are taken to be nonzero.[32] Since these coefficients imply a faster attachment to the protofilament where the stronger lateral bond is created, and conversely, a slower dissociation where a stronger lateral bond is to be broken, it is necessary to investigate the degree of significance of their effects on the growth velocities of the microtubules. Two different schemes are employed for this part of the investigation. First, we consider the case where all f_i are positive. In the second scheme, f_i are randomly chosen to be positive or negative. It follows from Fig. 4 that the inclusion of f_i, whether they are all positive or positive and negative, produces results qualitatively similar to the case where all $f_i=0$ and the effects of activation energy coefficients on the specific polymerization/depolymerization processes are not significant. For this reason, we did not consider the effects of activation energy coefficients further in this work and assumed $f_i=0$.

We then calculated the mean growth velocities for the analytically intractable case of $N=13$ full model by varying the lateral energy parameter γ. The rates of attachment and detachment of the leading protofilament, R_a and R_d, are taken to be 8.3 and 355 s^{-1}, respectively, to be consistent with the work of Ref. 12 and we utilized them in the $N=13$ full model in order to calculate the range of lateral interactions that is significant for microtubule growth. The plot of various γ and their corresponding velocities can be seen in Fig. 5. It is found that γ ranges from 45 to 280, which corresponds to $-6k_BT \lesssim g_h \lesssim -3k_BT$. The same range of g_h was also found by VanBuren *et al.*[14] by using a simplified stochastic model of microtubule assembly dynamics. Note in Fig. 5 that outside the range of $-6k_BT \lesssim g_h \lesssim -3k_BT$, either no growth occurs or that the growth velocity plateaus so that no larger value of γ (correspondingly, no smaller value of g_h) has any significant effect on growth. It is important to note that this model, which includes only the effects of local geometries of the growing end of the biopolymer and the specific lateral interactions of the adjacent protofilaments, captures the essential physical properties of polymerization/depolymerization processes.

Another significant aspect of this study is the effect of

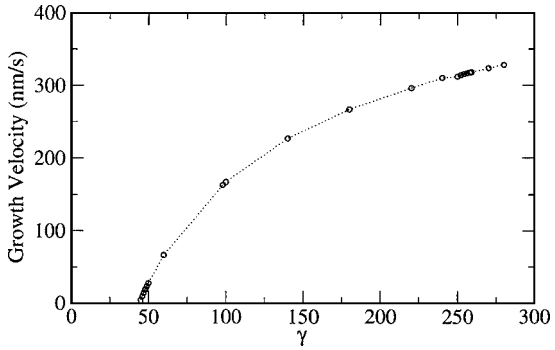

FIG. 5. Mean growth velocity as a function of the lateral energy parameter γ for the case of $N=13$ full model. The range of lateral energy parameter corresponds to values of g_h: $-6k_BT \lesssim g_h \lesssim -3k_BT$.

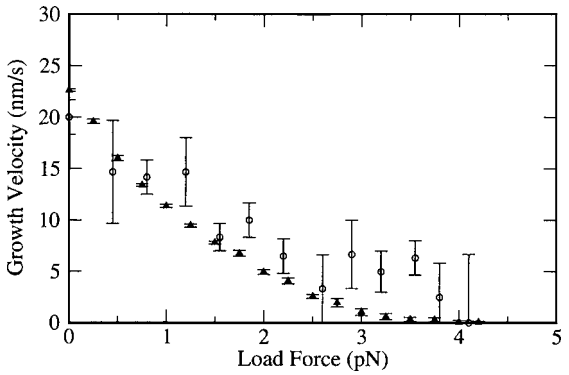

FIG. 6. Force-dependent mean growth velocity as a function of external (load) force for the case of $N=13$ full model. (▲) shows this work. (○) are experimental results (Ref. 5).

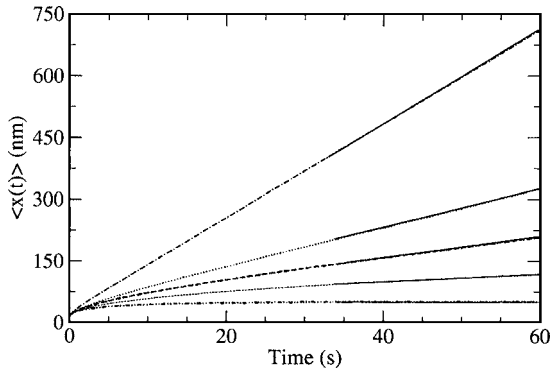

FIG. 7. Mean length $\langle x(t)\rangle$ for various values of load force F as a function of time t. The lines correspond, from top to bottom, to $F=1$ pN, $F=2$ pN, $F=2.5$ pN, $F=3$ pN, and $F=4$ pN.

the forces generated by growing microtubules. These forces are crucial for various forms of mechanisms of cellular motility and cellular transport.[2,3,5] For example, assembling microtubules are believed to exert pushing forces on chromosomes during mitosis. Experimentally, these forces are determined by putting the growing microtubules under external loads (*in vitro*), thus retarding growth. The source of external loads are hard walls and/or optical trap systems.[5,6] In order to consider the effect of external loads, the rate equations must be modified. The force F acts locally only on the leading protofilament, and the microtubule produces work equal to $F(d-a_i)$ when a subunit is attaching to protofilament i. The rates are adjusted as follows:[12]

$$r_{ai}(F) = r_{ai}(0)e^{-[\theta_i^+ F(d-a_i)/k_BT]}, \tag{30}$$

$$r_{di}(F) = r_{di}(0)e^{+[\theta_i^- F(d-a_i)/k_BT]}, \tag{31}$$

where $r_{ai}(0)$ and $r_{di}(0)$ are the rates [cf. Eqs. (10) and (11)] without the external force F.

For Eqs. (30) and (31), $(d-a_i)$ is the microtubule length change for a monomer binding to the protofilament i. θ_i^+ and θ_i^- are load distribution factors which reflect how the external force affects the activation energy for attachment and detachment processes of the subunit.[10,12,33] These load distribution factors may be positive or negative. However, since the load serves to retard growth, the overall constraint is[12]

$$\sum_{i=1}^{N} (\theta_i^+ + \theta_i^-) = 1. \tag{32}$$

By modifying the rates this way, a force-velocity relationship for $N=13$ case is obtained in Fig. 6 for the full model. Figure 7 shows the mean length $\langle x(t)\rangle$ of the microtubule for different values of load force F as a function of time t, and the slopes of the lines at large times represent the velocities in Fig. 6. It can be seen in Fig. 7 that the slopes become more horizontal as the load force F increases. The experimentally obtained force-velocity curve of microtubules[5] has been fitted with theoretical models.[9,10,12] Whereas previous theoretical fits overestimate the "stalling" force F_s [the value of force for which the mean growth velocity approaches zero due to the hindrance of polymerization by the external force (or load force),[8,10,12]] note in Fig. 6 that our simulation predicts $F_s \approx 4$ pN, very close to the experimental value of 4.1 pN.[5] The parameters used in Fig. 6 are $d=8.2$ nm, $a=0.63$ nm, $R_a=8.3\ s^{-1}$, $R_d=355\ s^{-1}$, and $\gamma=48.27$. The set of load distribution factors used in the simulations were equal in value for all protofilaments except 1 and 13, and satisfies Eq. (32). They are 0.249 45 for $\theta_1^{\pm}$ and $\theta_{13}^{\pm}$, and 0.0001 for $\theta_2^{\pm}-\theta_{12}^{\pm}$.[34] This reflects the fact that the load force affects the protofilaments at the seam (1 and 13) much more heavily than the other protofilaments. The value of γ was estimated from Fig. 5 and corresponds to the experimentally determined growth velocity (without load force) of 1.2 μm/min $\approx$ 20 nm/s. In reality, $a=0.96$ nm for microtubules. However, we used $a=0.63$ nm in our simulations for the purpose of developing a method and checking its validity on the simplified geometry (see Sec. II). Although we employed this simplified geometry in our simulations, the results for realistic geometry are expected to be similar to the present results since the essential physics is the same. In addition, even though the computed force-dependent growth velocity decays faster than the experimentally observed velocity, the estimated stalling force of 4 pN is almost identical to the real value. Such a fast decay in velocity can be attributed to the simplified geometry, and our method may be the ground for further improvement and predictions.

V. CONCLUSIONS

Monte Carlo simulations were performed for predicting the growth velocities of rigid biopolymers. The effects of the complex structure of the growing end, the geometrical properties, and the lateral interactions between adjacent protofilaments on the growth dynamics of rigid biopolymers were explicitly taken into account. The simulations successfully reproduced the mean growth velocity ratios of the analytical model for the $N=2$ case, and the one-layer approximation was found to be in excellent agreement with the full model, especially for larger lateral displacements a/d. The $N=13$ simulation displayed a similar qualitative behavior as the $N=2$ case, i.e., the ratio of velocities approached 1 for higher lateral energy parameter γ. However, the obtained ratio was 0.907 for $\gamma=1$ as opposed to the value of 0.5 for the $N=2$ case. The simulations indicate that the one-layer approximate model is a good representation of the growth dynamics of multiprotofilament biopolymers. Simulations for nonzero ac-

tivation energy coefficients in the $N=2$ case were also performed. As expected, both cases (f_i is only positive or f_i is both positive and negative) produced qualitatively similar results to the $f_i=0$ case, which means that the effects of activation energy coefficients on the specific polymerization/depolymerization processes are not significant.

For the $N=13$ full model, which is relevant to microtubules, we calculated a range of lateral free energies that affects the growth velocities of microtubules significantly. We found that the lateral free-energy parameter γ ranges from 45 to 280, which corresponds to $-6k_BT \lesssim g_h \lesssim -3k_BT$. By considering only the effects of local geometries of the growing end of the microtubule and the specific lateral interactions of the adjacent protofilaments, we obtained a reasonable range of lateral free energies.[14] Furthermore, we were able to produce a force-velocity relationship that is comparable to experimental results[5] by performing simulations for the case of $N=13$ full model. The lateral energy parameter γ that was used in these simulations corresponds to a growth velocity of 20 nm/s (when no external load force is applied), and the force-dependent curve thus obtained is in good accord with experimental measurements. The stalling force was estimated to be $F_s \approx 4$ pN, which is slightly less than the experimentally determined value of $F_s=4.1$ pN. This difference can be attributed to the simplified geometry that was employed in our simulations. However, the discrepancy in the stalling force of ~ 0.1 pN is less than the overestimated values [$F_s=4.3$ pN,[10] $F_s=5.5$ pN[12]] of previous theoretical predictions.

Continuing in this course, future work will be focused on obtaining and refining the velocities for multiprotofilament cases, as well as improving the force-velocity relation. Such improvements could include allowing for hydrolysis effects and nonequal load distribution factors for the protofilaments. Calculating the dispersion, or the effective diffusion constant of length fluctuations, will provide a better understanding of the dynamics of growth. An expansion of the simple model to incorporate the apparently weaker interactions at the polymer lattice seam and the hydrolysis effects would bring the model closer to real systems. Note that this method is not limited to microtubules, but may be applied to other rigid biopolymer dynamics.[35] In addition, the application of this approach might suggest an explanation of the mechanism by which motor proteins modulate biopolymer dynamics, as they are known to alter the exchange of tubulin subunits at growing ends.[3,36]

ACKNOWLEDGMENTS

We appreciate the interest of Professor M. E. Fisher and Professor V. I. Manousiouthakis. One of the authors (J.S.) gratefully acknowledges the Eugene Cota Robles Fellowship of UCLA Graduate Division. Another author (G.O.) acknowledges support by Intel® Higher Education Program Equipment Grant and UCLA startup funds. Another author (A.B.K.) acknowledges support from the Camille and Henry Dreyfus New Faculty Awards Program (under Grant No. NF-00-056), from the Welch Foundation (under Grant No. c-1559), and from the US National Science Foundation through Grant No. CHE-0237105.

[1] H. Lodish, A. Berk, L. S. Zipursky, P. Matsudaira, D. Baltimore, and J. Darnell, *Molecular Cell Biology*, 4th ed. (Freeman, New York, 2000).
[2] A. Desai and T. J. Mitchison, Annu. Rev. Cell Dev. Biol. **13**, 83 (1997).
[3] J. Howard and A. A. Hyman, Nature (London) **422**, 753 (2003).
[4] L. Evans, T. Mitchison, and M. Kirschner, J. Cell Biol. **100**, 1185 (1985).
[5] M. Dogterom and B. Yurke, Science **278**, 856 (1997).
[6] J. W. Kerssemakers, M. E. Janson, A. van der Horst, and M. Dogterom, Appl. Phys. Lett. **83**, 4441 (2003).
[7] I. Fujiwara, S. Takahashi, H. Tadakuma, T. Funatsu, and S. Ishiwata, Nat. Cell Biol. **4**, 666 (2002).
[8] G. S. van Doorn, C. Tanase, M. Mulder, and M. Dogterom, Eur. Biophys. J. **29**, 2 (2000).
[9] A. Mogilner and G. Oster, Eur. Biophys. J. **28**, 235 (1999).
[10] A. B. Kolomeisky and M. E. Fisher, Biophys. J. **80**, 149 (2001).
[11] H. Bolterauder, H. J. Limbach, and J. A. Tuszynski, J. Biol. Phys. **25**, 1 (1999).
[12] E. B. Stukalin and A. B. Kolomeisky, J. Chem. Phys. **121**, 1097 (2004).
[13] Note that Mogilner and Oster (Ref. 9) indirectly included the interactions of the protofilaments by incorporation of a "subsidy effect."
[14] V. VanBuren, D. J. Odde, and L. Cassimeris, Proc. Natl. Acad. Sci. U.S.A. **99**, 6035 (2002).
[15] B. Derrida, J. Stat. Phys. **31**, 433 (1983).
[16] E. B. Stukalin and A. B. Kolomeisky, J. Chem. Phys. **122**, 104903 (2005).
[17] T. Hill, *Linear Aggregation Theory in Cell Biology* (Springer, New York, 1983).
[18] Note that the fraction of lateral interactions is equal to 1 for either side of protofilament i if the tip of protofilament i is at a distance greater than d from the adjacent protofilaments.
[19] D. J. Odde, Biophys. J. **73**, 88 (1997).
[20] For the leading protofilament, the activation energy coefficient is zero since there are no lateral interactions ($m_i=0$).
[21] R. J. Glauber, J. Math. Phys. **4**, 294 (1963).
[22] H. Müller-Krumbhaar and K. Binder, J. Stat. Phys. **8**, 1 (1973).
[23] A. B. Bortz, M. H. Kalos, and J. L. Lebowitz, J. Comput. Phys. **17**, 10 (1975).
[24] K. A. Fichthorn and W. H. Weinberg, J. Chem. Phys. **95**, 1090 (1991).
[25] K. Binder and M. H. Kalos, *Monte Carlo Methods in Statistical Physics* (Springer, Berlin, 1979).
[26] D. T. Gillespie, J. Comput. Phys. **22**, 403 (1976).
[27] D. T. Gillespie, J. Comput. Phys. **28**, 395 (1978).
[28] D. T. Gillespie, Physica A **188**, 404 (1992).
[29] D. Frenkel and B. Smit, *Understanding Molecular Simulation from Algorithms to Applications*, 2nd ed. (Elsevier, San Diego, 2002).
[30] M. P. Allen and D. J. Tildesly, *Computer Simulation of Liquids* (Oxford University Press, New York, 1987).
[31] Note that for the "one-layer" model, states that violate $a_i \leq d$ are assigned zero probability.
[32] During an elementary step (attachment or detachment) the lateral interactions are calculated and f_i is given a random value within the appropriate range, cf. Eqs. (12) and (13).
[33] A. B. Kolomeisky and M. E. Fisher, Biophys. J. **84**, 1642 (2003).
[34] By performing simulations with different sets of load distribution factors, the values of 0.249 45 (for $\theta_1^{\pm}$ and $\theta_{13}^{\pm}$) and 0.0001 (for $\theta_2^{\pm}-\theta_{12}^{\pm}$) were chosen to produce force-dependent growth velocities that have the best possible agreement with experimental measurements (Ref. 5).
[35] M. Busch, M. Müller, and M. Wułkow, Chem. Eng. Technol. **26**, 1031 (2003).
[36] A. W. Hunter and L. Wordeman, J. Cell. Sci. **113**, 4379 (2000).